The Role of the Characteristic Line in Static Soil Behavior

Ibsen, Lars Bo; Lade, Poul V.

Published in:
Proceedings of the 4th International Workshop on Localization and Bifurcation Theory for Soil and Rocks

Publication date:
1998

Document Version
Publisher's PDF, also known as Version of record

PROCEEDINGS OF THE FOURTH INTERNATIONAL WORKSHOP
ON LOCALIZATION AND BIFURCATION THEORY FOR SOILS AND ROCKS
GIFU/JAPAN/28 SEPTEMBER - 2 OCTOBER 1997

Localization and Bifurcation Theory for Soils and Rocks

Edited by
TOSHIHISA ADACHI & FUSAO OKA
Kyoto University, Japan
ATSUSHI YASHIMA
Gifu University, Japan

OFFPRINT

A.A. BALKEMA / ROTTERDAM / BROOKFIELD / 1998

Localization and Bifurcation Theory for Soils and Rocks, Adachi, Oka & Yashima (eds)

The role of the characteristic line in static soil behavior

Lars Bo Ibsen
Department of Civil Engineering, Aalborg University, Denmark
Poul V. Lade
Department of Civil Engineering, The Johns Hopkins University, Baltimore, Md., USA

ABSTRACT: Experiments have been performed on several types of sand, and the data have been analyzed to study the characteristic line of sand behavior. The definition of this line is reviewed, it is compared with the phase transformation line, and the factors that may affect the characteristic line have been investigated. These include the relative density, the minor and the intermediate principal stresses, the stress path and the effect of nonhomogeneous and localized strains. The relation of the characteristic line to other features of soil behavior are explained in view of experimental results. In particular, its determination from drained, static triaxial compression tests is explained and its significance for undrained conditions is demonstrated.

1 INTRODUCTION

Volume changes are important for the behavior of soils whether under drained or undrained conditions. Volume changes can be compressive or expansive in nature. Expansive or dilative volume changes are most pronounced for dense sands at low confining pressures and high stress levels approaching failure. The transition from compressive behavior observed at lower stress levels to dilative behavior at high stress levels occurs along a straight line through the origin of the stress space. For drained tests, this line is referred to as the characteristic line.

In elasto-plasticity models the characteristic line, evaluated from $p' = const$ tests, corresponds to the point on the plastic potential surface where the plastic strain increment vector is perpendicular to the p'- axis or the hydrostatic axis. This state is therefore comparable to the similar point on the yield surface at which the normal is perpendicular to the hydrostatic axis. This indicates the point at which sand may become unstable, as explained in detail elsewhere (Lade 1995). Thus, the characteristic line plays a similarly important role for the plastic potential surface as the instability line plays for the yield surface. Both lines are shown on the diagram in Figure 1. The behavior of soils is greatly influenced by and may be explained in view of the relative locations of these two lines. For sands the two lines are distinctly separate, while for normally consolidated, insensitive clays the two lines coincide, and they also coincide with the critical state or ultimate state line.

Experiments have been performed to study the factors that influence the location of the characteristic line in drained and undrained tests for various types of sand. These factors include the relative density, the minor principal stress, the intermediate principal stress, the influence of stress path and the effect of nonhomogeneous and localized strains. The

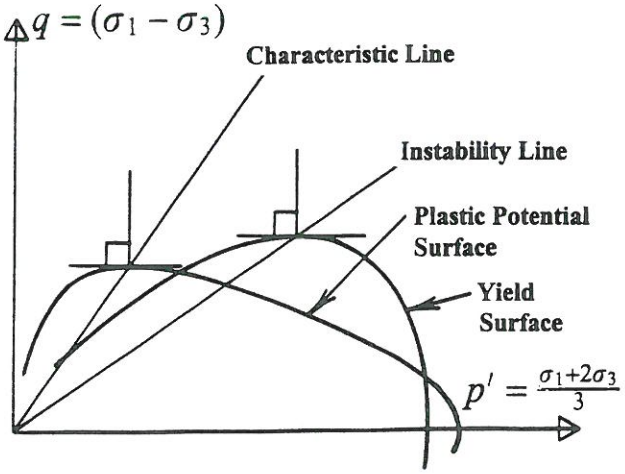

Figure 1. Comparison of characteristic and instability lines.

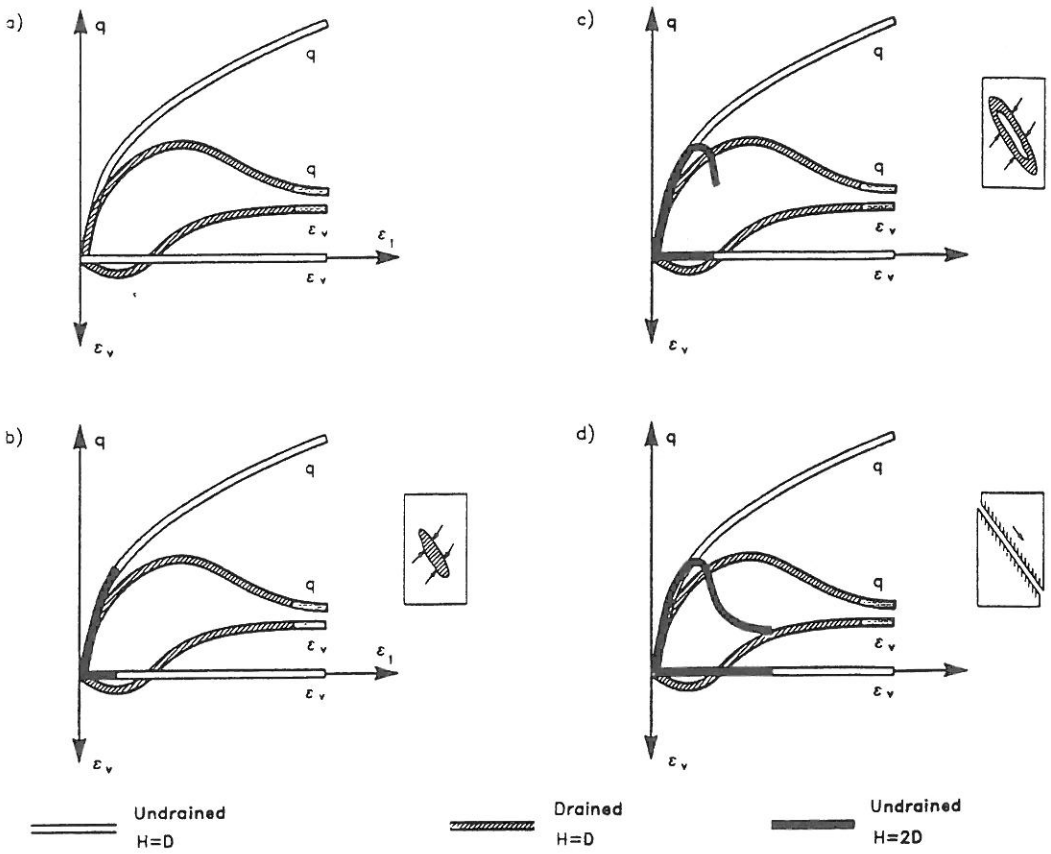

Figure 2. The consequence of an undrained test run on a specimen with double height. (a) Drained and undrained test run under homogeneous strain conditions. (b) Development of the locally weakened zone in which the shear plane subsequently is formed. (c) The drained zone dominates the performance curve. (d) Two practically solid bodies sliding past each other (H = height and D = diameter of the specimen).

relation of the characteristic line to other features of soil behavior is explained and illustrated with experimental data.

2 EFFECT OF LOCALIZED STRAINS

The relative height of a triaxial specimen does not play any role in the stress distribution inside the specimen bounded by smooth end platens, but severe nonuniformities in strain can develop if the height of the specimen is greater than the diameter, and lubrication is not employed (Jacobsen 1967, Lade 1982). After dismantling the the triaxial setup - especially for tests on firm soil - the shape of a tall specimen usually shows failure as a narrow rupture zone, a shear band, where two practically solid bodies have slid past each other, as shown in Figure 2d. At this stage of the test, the shear deformations and volume changes occur in the localized zone, and the soil properties measured do not refer to the whole specimen - as normally assumed - but only to the material sheared in this narrow failure zone. As a consequence the vertical deformation is dominated by the movements in this zone, and the shear strains should be calculated relative to the height of the localized zone and not to the height of the entire specimen. Unfortunately, the height of the localized zone is unknown, and the height of the specimen is therefore often employed for calculation of "strains." Consequently, the stress-"strain" curve will be too short, and the compression phase may only be correct at the very beginning of the test, as shown in Figure 3a. The measured curve does not compare favorably with the stress-strain curve obtained from a test performed with homogeneous stress and strain conditions in which uniform strains are forced to occur. Homogeneous conditons may be achieved by performing triaxial compression tests with smooth cap and base and with height equal to diameter.

If the heterogeneous strain state is permitted to develop, the volume changes will also be concentrated in the narrow localized zone and only small volume changes occur in the sand mass outside the shear band. Once the sand in the localized zone has expanded to the critical void ratio, no further volume changes take place in the specimen. Figure 3b indicates that the rate of dilation of the tall specimen

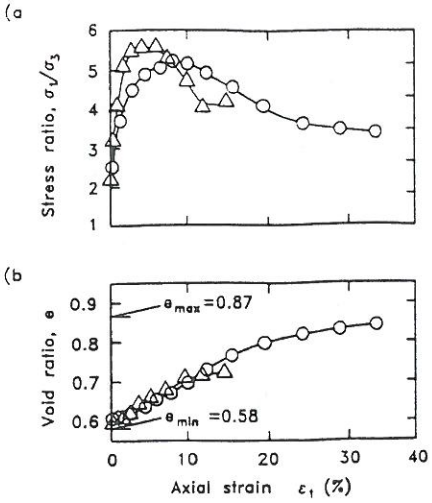

Figure 3. Comparison of stress-strains and void changes in triaxial compression test on dense Santa Monica Beach sand. I_D = 0.9 with H/D = 1.0 marked O, and H/D = 2.7 (and no lubrication) marked Δ.

has essentially ceased at about 12 % axial strain, whereas in the specimen with uniform strains, volume changes occur and continue even at 35 % strain. Because the volume change measured in a triaxial test represents the average volume change for the entire specimen, the final average void ratio for the tall specimen is seen to be much smaller than the actual critical void ratio for the sand, at a given confining pressure. However, it is clear that the nonuniformities in strain influence the stress-strain curve from the very beginning of the test, as also shown in Figure 3a. Note that the quantity known as the relative density is now referred to as the density index, I_D, in Figure 3.

The tall specimen's incapability to produce uniform deformation conditions throughout the test also has considerable influence on the results of undrained tests. Test results of drained and undrained triaxial tests performed on specimens with homogeneous stress and strain distributions are shown in Figure 2a. The same sand was also tested in an undrained triaxial test with the height of the specimen equal to twice the diameter, as shown in Figure 2b. Initially the two stress-strain curves from the undrained tests coincide. As the deviator stress q increases, the soil will try to expand. Under homogeneous conditions this expansion is impossible since the drains are closed. The resulting pore water suction will increase and hold the grain structure together. But in the tall specimen the deformation is not homogeneous, and some local zones will dilate and others will contract, resulting in zero overall volumetric strain. Inside the specimens water will flow from the zones that contract to the zones that dilate, as shown on the insert in Figure 2b. As a consequence, the test is not truly undrained, even though the overall volume of the whole specimen is kept constant. The stress-strain curve corresponding to these opposing volume change tendencies begin to deviate from the curve obtained from the uniform strain test as the zones with non uniform strains develop into more distinct localized zones, as illustrated on the insert in Figure 2c. Consequently, the inner drainage of some portions of the tall specimen causes the externally measured stress-strain curve to resemble the curves from the fully drained tests shown in Figure 3a. Critical state conditions develop inside the localized shear zone as the test continues. A shear band develops, and two practically solid bodies slide past each other, as indicated on the insert in Figure 2d. This limits the full development of negative pore pressure, and the shear strengths from such tests are consequently too low.

3 SHEAR STRENGTH OF SAND

The typical variation of drained shear strength of sand with mean effective stress is illustrated schematically in Figure 4. For a sand with a given initial density, the peak friction angle, φ_{peak}, consists of two components. One from the basic friction between sand particles modified for contributions from rearrangement of particles at constant volume. The resulting friction angle is referred to as the critical friction angle, φ_{crit}. The second component derives from the dilation of the sand during shear, ψ_{peak}. This relation can be expressed as:

$$\varphi'_{peak} = \varphi'_{crit} + \psi_{peak} \qquad (1)$$

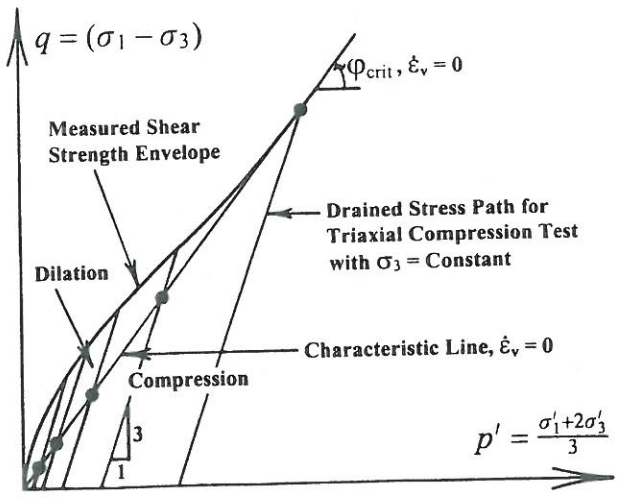

Figure 4. Variation of drained shear strength envelope for sand with confining pressure.

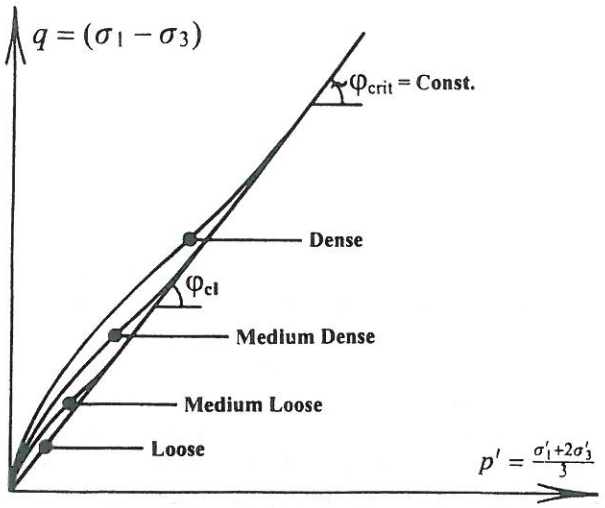

Figure 5. Variation of drained shear strength envelope for sand with relative density.

The dilation is suppressed at higher pressures due to crushing, and the resulting strength component therefore reduces to zero at very high pressures. Thus, a curved failure surface is observed. Experiments on sands have shown that both the contribution from dilation and the range of confining pressures in which dilation occurs reduce with decreasing relative density, as shown schematically in Figure 5.

4 THE CHARACTERISTIC LINE

The separation between the region of compression and the region of dilation for drained tests on sand occurs at the characteristic state at which the rate of volume change is zero, $\delta\varepsilon_v/\delta\varepsilon_1 = 0$ (Luong 1982), as shown schematically in Figure 6. Characteristic states occur at the transition from compression to dilation, and these states are located on a line, the characteristic line, through the stress origin. The slope of the characteristic line may be described by an angle, φ_{cl}. The characteristic state and the critical state are very similar, as discussed by Luong (1982). For loose sand and sand at high confining pressure, $\delta\varepsilon_v/\delta\varepsilon_1 = 0$is reached at the critical state. The critical state is therefore the same as the characteristic state, and it occurs at failure for sand that compresses during shear. For dense sand or sand at low confining pressure, the characteristic state is reached at small strain magnitudes, as indicated in Figure 6, while the critical state is reached at large strains.

The characteristic line divides the stress space into two subspaces in which the stress combinations lead to different deformation mechanisms.

Below the characteristic line the stress combinations lead to contraction, i.e. $\delta\varepsilon_v > 0$.

Above the line the stress combinations lead to dilation, i.e. $\delta\varepsilon_v < 0$.

Below the characteristic line the resistance to deformation is governed by sliding friction due to microscopic interlocking depending upon surface roughness of the particles or interlocking friction between particles. According to Luong (1982), the resistance is due to pure friction, and the characteristic state is described by an intrinsic parameter, the characteristic angel, φ_{cl}, for a given sand. In the subspace situated between the failure envelope and the characteristic line the resistance to deformation is governed by disrupture of interlocking and volumetric dilation.

4.1 Effects of Relative Density and Minor Principal Stress

The characteristic angles for drained triaxial compression tests on Aalborg University sand No.1 (Ibsen and Bødker 1994) and Lund sand No.0 (Ibsen and Jakobsen 1996) at four density indices I_D are shown in Figures 7 and 8. The index properties of these sands are shown in Table 1.

These experiments were performed on specimens with height equal to diameter and with lubricated ends. The specimens were prepared by pluviation and carefully saturated in total vacuum (approx. -98 kPa). This technique ensured homogeneous and fully saturated specimens. All specimens were therefore pre-consolidated to 100 kPa during the preparation.

Table 1. Index Properties.

Property	Aalborg University sand No. 1	Lund sand No. 0
d_{50} mm	0.14	0.4
C_U	1.78	1.7
d_s	2.65	2.65
e_{max}	0.85	0.82
e_{min}	0.55	0.55

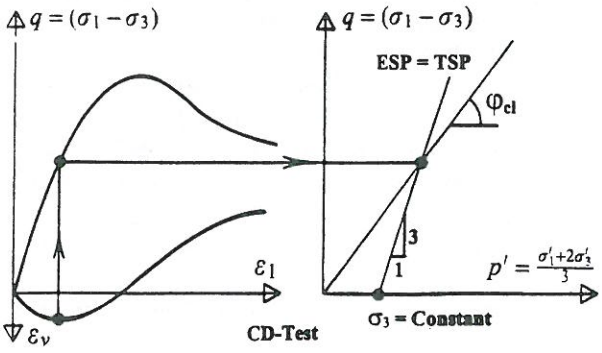

Figure 6. Schematic diagram of characteristic state in drained triaxial compression test on sand.

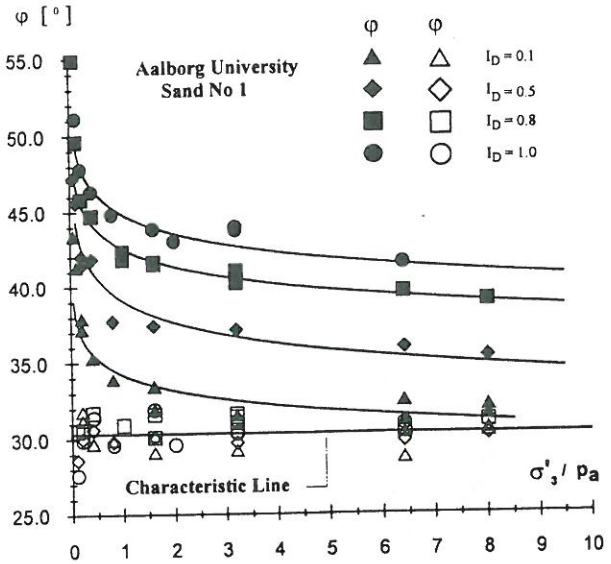

Figure 7. Characteristic angles obtained from triaxial compression tests on Aalborg University sand No. 1.

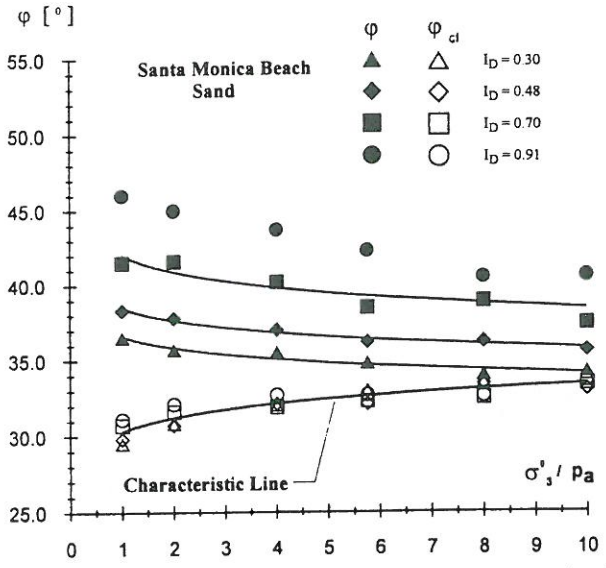

Figure. 9 Characteristic states obtained from triaxial compression tests on Santa Monica Beach sand.

The experiments in these two tests series, in which the density index, I_D, varied from 0.01 to 1.00, shows that the characteristic angle φ_{cl} is constant and independent of (1) density index for a given sand, and (2) confining pressure or minor principal stress. These observations were also made by Loung (1982). As discussed in connection with Figure 16, the determination of the stress state at which $\delta\varepsilon_v = 0$ is not necessarily very accurate, because the volume change curve is relatively flat near the characteristic state, while the stress state varies considerably. Therefore, the determination of the characteristic stress points shows some scatter. The characteristic angle for Aalborg University sand No. 1 is found to be $\varphi_{cl} = 30.3^0$ and for Lund sand No.0 it is $\varphi_{cl} = 29.5^0$. These angles are determined according to the definition used by Luong (1982).

4.2 Effects of Specimen H/D-Ratio

The characteristic stress states corresponding to $\delta\varepsilon_v = 0$ for triaxial compression tests on Santa Monica Beach sand at four density indices (Lade and Prabucki 1995) are shown in Figure 9. These experiments were performed on specimens with height-to-diameter ratio $H/D = 2.65$ and with lubricated ends. They also show that the characteristic angle, φ_{cl}, is independent of density index for a given sand, but

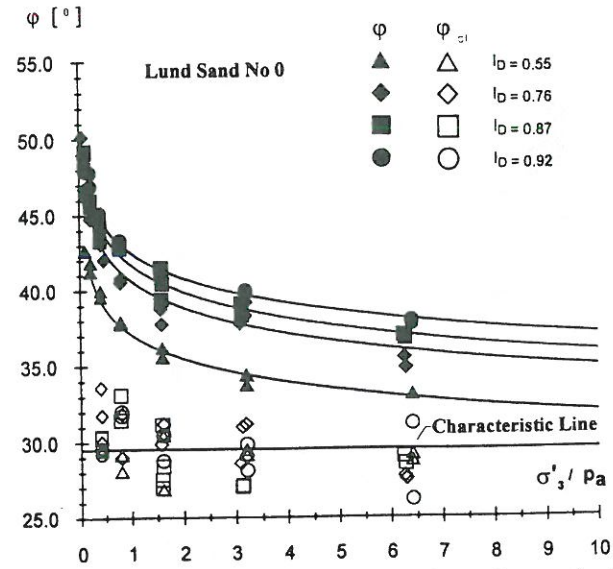

Figure 8. Characteristic angles obtained from triaxial compression tests on Lund sand No. 0.

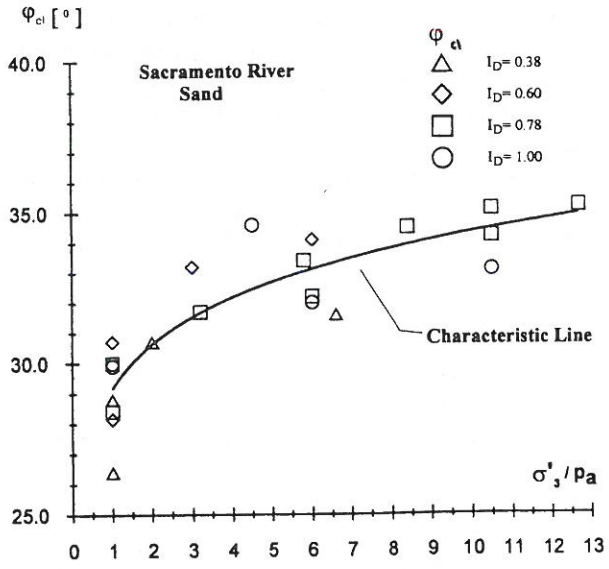

Figure. 10 Characteristic states obtained from triaxial compression tests on Sacramento River sand.

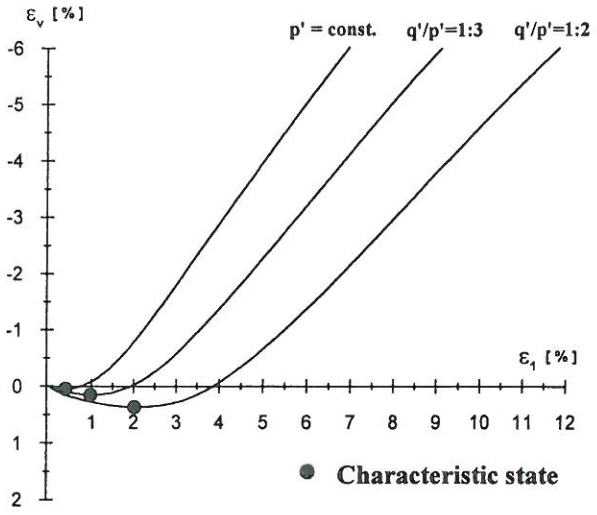

Figure 11. Volumetric curves obtained by stress path tests on Aalborg University sand No. 1, I_D = 1.00. Isotropic consolidated to $\sigma_3' = 200$ kPa before shearing.

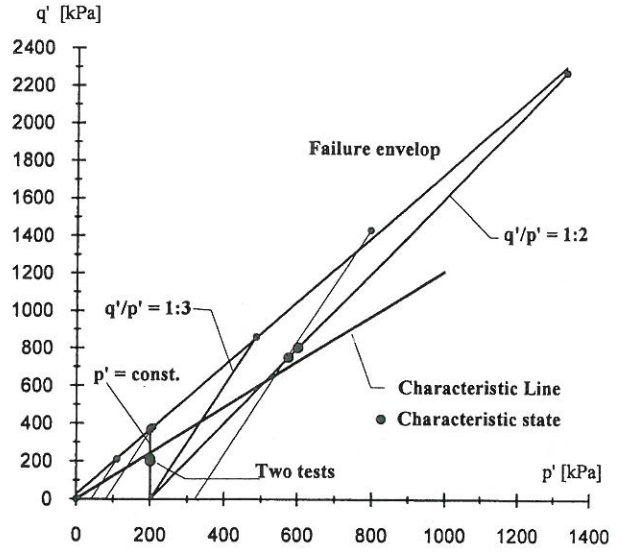

Figure 12. Stress paths employed in triaxial compression tests on Aalborg University sand No. 1, $I_D = 1.00$.

due to the development of nonuniformities in strains, the angle is found to vary slightly with the minor principal stress.

The characteristic angles for drained triaxial compression tests on Sacramento River sand (Lee 1965, Lee and Seed 1967) were also determined for four different density indices, and they are shown in Figure 10. These tests were performed on specimens with $D = 3.56$ cm and $H/D = 2.43$, and without lubricated ends. The data for Sacramento River sand shows more scatter than the other test series. Still the tests indicate that the characteristic angle is independent of density index. Due to the more pronounced nonuniformities in stress and strains, caused by rough end plates, the characteristic angles vary more with confining pressure than the data for Santa Monica Beach sand. It is therefore important to realize that the nonuniform deformations, which develop at very small strains, influence the measured characteristic angles and therefore the conclusions regarding the effect of the minor principal stress.

4.3 Effects of stress path testing

The characteristic stress state discussed above is that observed in conventional triaxial compression tests in which the stress path corresponds to constant confining pressure and $\delta q'/\delta p' = 1/3$. The volumetric strain curves from three triaxial test on Aalborg University sand No. 1 conducted with different stress path are shown in Figure 11. The tests were all performed on specimens with $I_D = 1.00$ and consolidated to a mean normal stress of $\sigma_3' = 200$ kPa before shearing. The corresponding stress path $\delta p' = const$, $\delta q'/\delta p' = 1/3$ and $\delta q'/\delta p' = 1/2$ are shown in Figure 12.

Contraction and dilation can be caused by application of shear stresses as well as by changes in the mean normal stress. In the constant p'-test the increment $\delta p'$ is zero and the elastic volumetric strain increment is therefore also zero. In this test the volumetric strains are caused entirely by shear stresses. The test shows shear-induced contraction in the beginning, and it is possible to define a characteristic state, as shown in Figure 11. As expected, the contraction becomes more pronounced as the stress

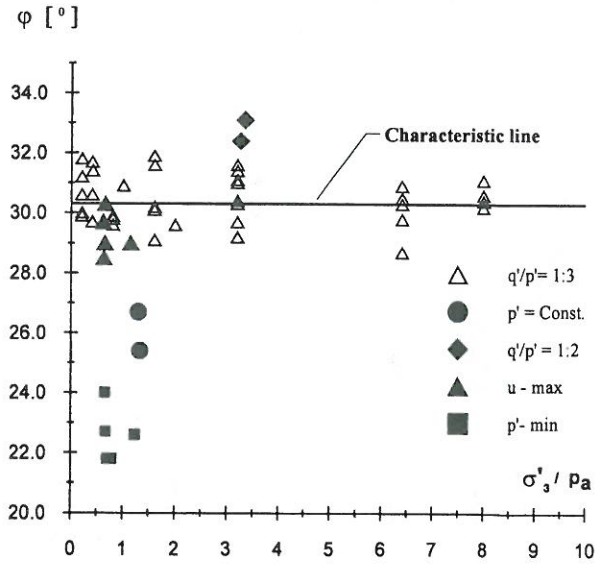

Figure 13. Angles of characteristic stress states, phase transformation stress states, and u_{max} stress states evaluated from drained and undrained triaxial tests on Aalborg University sand No 1.

ratio $\delta q'/\delta p'$ increases, and there are distinct differences between the characteristic states obtained from different stress paths, as clearly shown in Figure 11.

The characteristic stress states from the three volumetric strain curves are plotted in Figure 12. The characteristic line determined from the results in Figure 8 and two experiments for each of the conditions, $p' = const$ and $\delta q'/\delta p' = 1/2$, are also plotted in this diagram. The characteristic stress states from the $p' = const$ tests are located below and the stress states form the $\delta q'/\delta p' = 1/2$ are located above the characteristic line. The characteristic angle φ_{cl} from these four tests are also plotted in Figure 13. It is seen that φ_{cl} from the $p' = const$ tests is 26°, and it is 33° in the tests with the stress path $\delta q'/\delta p' = 1/2$. The characteristic angles are outside the general scatter of the $\delta q'/\delta p' = 1/3$ tests, and it appears from these experiments that the characteristic stress state and therefore the characteristic angle is a function of the stress path.

4.4 Effects of intermediate principal stress

The characteristic angles have also been obtained from drained cubical triaxial compression tests on dense and loose Monterey No.0 sand (Lade and Duncan 1973) and shown in Figure 14. The characteristic angles are affected by the intermediate principal stress in a similar fashion as the measured friction angles. Each b-value represents a different stress path in the stress space, and there does not seem to be any pronounced effect of density index on the characteristic angles. It is observed that for a given stress path, the characteristic stress states are independent of density index.

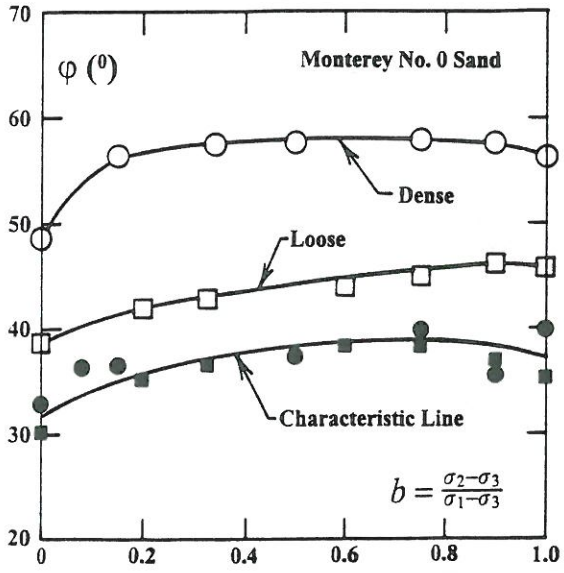

Figure 14. Characteristic angles obtained from cubical triaxial tests on Monterey No. 0 sand.

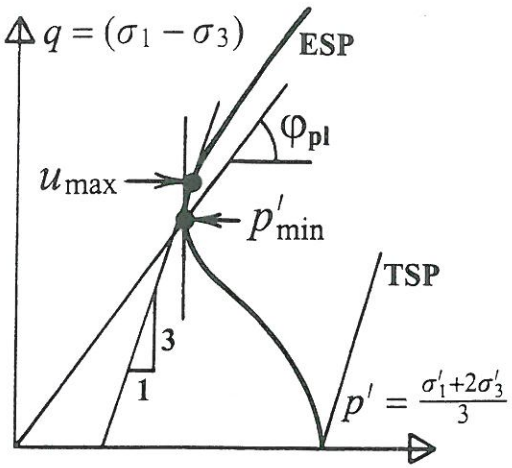

Figure 15 Schematic diagram of phase transformation state in undrained triaxial compression test on sand.

5 COMPARISON OF PHASE TRANSFORMATION AND CHARACTERISTIC STRESS STATES

The phase transformation stress state plays a similar role for undrained tests as the characteristic stress state plays for drained tests. Figure 15 shows a schematic illustration of the stress state at which phase transformation occurs along an effective stress path from an undrained test. It is the point at which "the stress path turns its direction in p'- q' space" (Ishihara et al. 1975), i.e. the point where the effective stress path has a "knee" and the effective mean normal stress reaches a minimum value p'_{min}. Ishihara et al. (1975) observed that for cyclic undrained triaxial tests "it is necessary for a sample to go at least once through this critical value in order to be taken to a completely liquefied state." In this sense, "the critical stress ratio may be considered as a threshold at which the behavior of sand as a solid is lost and transformed into that of a liquefied state."

Whereas the "knee" described above does not clearly define the location of the phase transformation point, the most consistent definition is one that is independent of the stress path. The phase transformation state is therefore best defined as the point at which the effective stress path has a vertical tangent.

At this point of the undrained test, the increment $\delta p'$ becomes zero, and the elastic volumetric strain increment, $\delta\varepsilon_v^e$, is therefore also zero. Consequently, the plastic volumetric strain increment, $\delta\varepsilon_v^p$, is also zero. This definition theoretically makes the characteristic and phase transformation states identical.

Inspection of the data in Figure 13 show that the characteristic angles obtained from $p' = const$ tests are slightly higher than the angles defining the phase

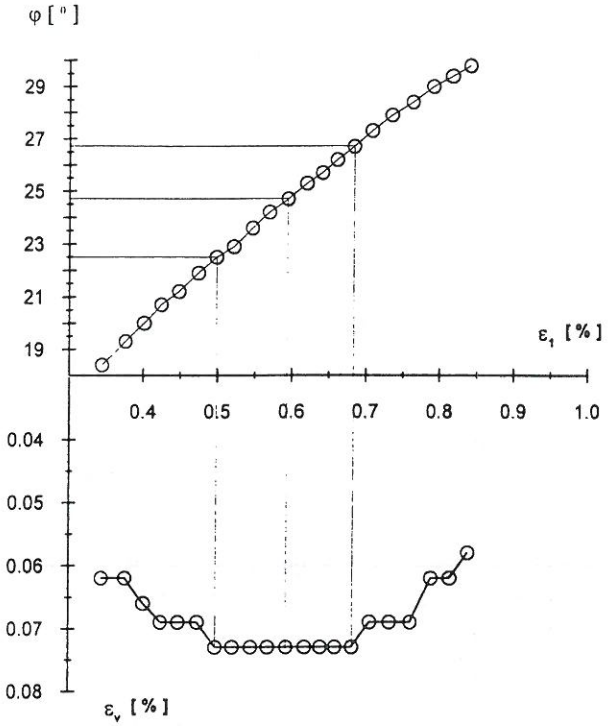

Figure 16. The measured points used to define the characteristic stress state in a p' = constant triaxial test run on Aalborg University sand No 1. I_D = 1.00.

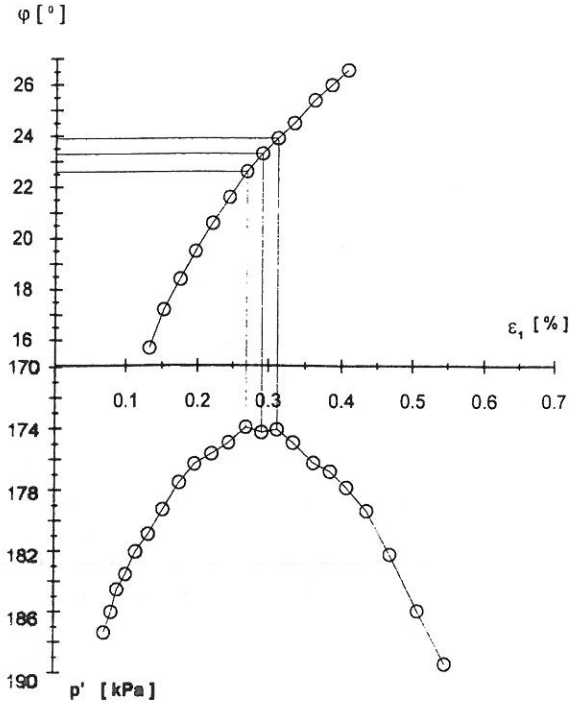

Figure 17. The measured points used to define the phase transformation stress state in a CU triaxial test performed on Aalborg University sand No 1 with I_D = 1.00.

transformation states. It was expected that the characteristic angle from $p' = const$ tests and the angle of the phase transformation states would be the same, because both stress states are characterized by having $\delta\varepsilon_v^e = 0$. However, the conditions defining the two stress states are not exactly identical. In the undrained test, the total volumetric strain is zero and the elastic and plastic volumetric strains therefore have to compensate for each other, i.e. $\varepsilon_v^e = -\varepsilon_v^p$, while $\varepsilon_v^e = 0$ and $\varepsilon_v^p \neq 0$ in the drained test.

In Figures 16 and 17 the points used to define the characteristic and phase transformation stress states are shown for tests performed on Aalborg University sand No. 1 with I_D = 1.00. Figure 16 shows that the transition zone in which $\delta\varepsilon_v = 0$ starts at φ = 22.5° and ends at φ = 26.7°. Previously, and according to Luong (1982), the characteristic stress state has been defined as the mean value in this transition zone producing φ_{cl} = 24.6°. In comparison, the transition zone for the phase transformation state in the corresponding undrained test is much narrower.

Redefining the characteristic and phase transformation states as the states where $\delta\varepsilon_v$ and $\delta p'$ becomes zero for the first time, produces identical states, if simultaneously, the characteristic state is obtained from a $p' = const$ test, shown in Figures 16 and 17.

This new definition is used in evaluating the angles shown in Figure 18. The test data are identical with those shown in Figures 8 and 15 for I_D = 1.00. Using this definition, all the characteristic angles, evaluated from CD - tests performed with $p' = const$, become identical with the angles of the phase transformation states. The characteristic angles still show the same stress path dependency as before, while those evaluated from conventional triaxial tests are reduced from φ_{cl} = 30.3° to φ_{cl} = 28.8°.

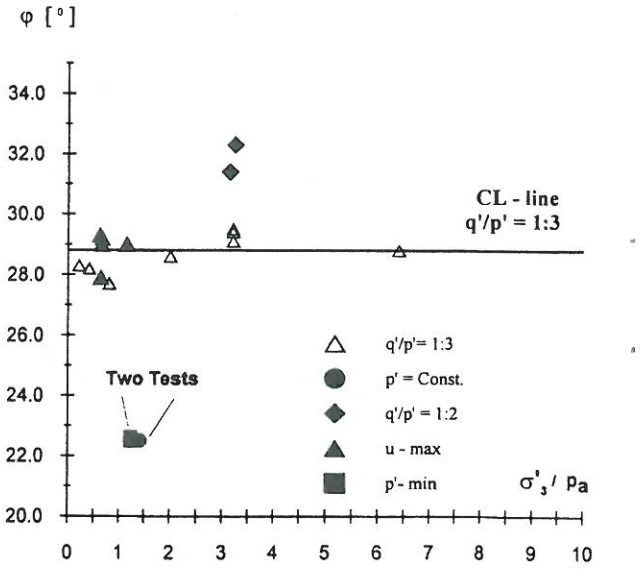

Figure 18. Angles of characteristic and phase transformation states defined as the stress state where $\delta\varepsilon_v$ becomes zero for the first time. The tests are run on Aalborg University sand No 1. I_D = 1.00.

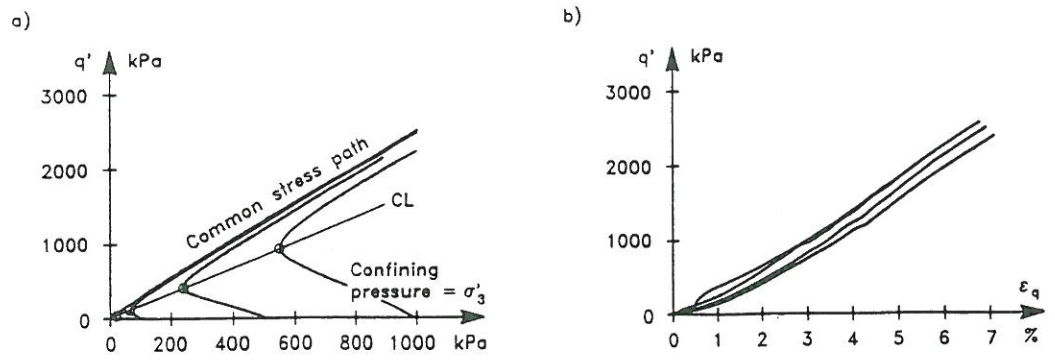

Figure 19. Results of four CU - tests performed on Lund sand No. 0 with $I_D = 0.78$. The tests were performed on specimens with equal height and diameter.

6 THE CHARACTERISTIC STATE FOR UNDRAINED CONDITIONS

Along the effective stress path in a undrained test the elastic and plastic volumetric strains have to compensate for each other, i.e. $\varepsilon_v^e = -\varepsilon_v^p$. It has been shown that changes in the effective mean normal stress p' affects both the elastic volumetric strain and the stress state where the soil goes from compression to dilation. In a conventional undrained triaxial compression test, in which the total stress path corresponds to $\delta q'/\delta p' = 1/3$, the phase transformation state does not correspond to the transition from compressive to dilative behavior, i.e. the point where the maximum pore water pressure u_{max} occurs.

The characteristic stress state, as defined by Luong (1982), together with the total stress path, controls the point where the maximum pore water pressure u_{max} occurs in an undrained test. During undrained shear, the pore pressure increases at first in order to prevent the sand from contraction, i.e. $\delta u > 0$. When the deviator stress approaches the characteristic state $\delta u \to 0$. The results of four undrained triaxial tests, shown in Figure 19, indicate that the stress states where $\delta u = 0$ are located on the characteristic line. If q increases further, the effective stress path is located in the subspace which is characterized by dilation. In order to prevent dilation, the pore pressure generation becomes negative, i.e. $\delta u < 0$, as shown in Figure 19a. If the effective stress path in figure 19a is plotted in a $p' - q$ diagram, the stress state corresponding to maximum pore water pressure u_{max} will occur slightly later than the phase transformation stress state, as indicated in Figure 15.

Stress states corresponding to u_{max} from five undrained tests performed on Aalborg University sand No. 1 with I_D = 1.00, 0.80 and 0.51 are shown in Figure 18. It is seen that u_{max} corresponds to the characteristic stress states for the tests conducted with the stress ratio $\delta q'/\delta p' = 1/3$. It is also recognized that the stress state where u_{max} occurs is quite different from the phase transformation stress state corresponding to p'_{min}.

7 CONCLUSION

In this paper, the characteristic state is redefined as the stress state where $\delta\varepsilon_v$ becomes zero for the first time in a test with $p' = const.$ Further, the phase transformation state is defined as the state where $\delta p'$ becomes zero for the first time. As a consequence, the characteristic and phase transformation lines become identical. These definitions are mutually consistent, and they may therefore be useful in controlling the plastic potential function for description of plastic volume changes of soils.

In comparison, the characteristic angle defined by Luong (1982) is not an intrinsic parameter, independent of stress path, and it not useful for development of elasto-plasticity models.

The characteristic line has been studied in view of experimental results from drained and undrained triaxial compression tests and cubical triaxial tests on different sands Experiments have shown, that the density index and the minor principal stress have little to negligible influence on the location of the redefined characteristic line and the characteristic angle is therefore unique for a given sand.

It is also shown that nonuniform deformations, which develop at very small strains in tall specimens, may influence the measured characteristic angles and the conclusions regarding the effect of the minor principal stress. It is therefore recommended to determine the characteristic and the phase transformation states from experiments with uniform stress and strain states. These are best produced in tests on specimens with height equal to diameter and lubricated ends.

REFERENCES

Ibsen, L.B. and Bødker, L. 1994. Baskarp Sand No. 15. *Data Report 9301*, Soil Mechanics Laboratory, Aalborg University, Denmark.

Ibsen, L.B. and Jakobsen, F.R. 1996. Lund Sand No. 0, *Data Report 8401, 8402, 8801 & 8901,* Soil Mechanics Laboratory, Aalborg University, Denmark.

Ibsen, L.B 1995. Static and dynamic strength of sand. *Eleventh European Conference on Soil Mechanics and Foundation Engineering*, 29 May - 1 June.

Ishihara, K., Tatsuoka, F. and Yasuda, S. 1975. Undrained deformation and liquefaction of sand under cyclic stresses. *Soils and Foundations,* 15:1, 29-44.

Jacobsen, M. 1967. The undrained shear strength of preconmsolidated boulder clay. *Proc. Geot. Conf.*, Oslo, I:119-122.

Lade, P. V. 1982. Localization effects in triaxial test on sand. *IUTAM Conference on Deformation and Failure of Granular Materials*. A.A. Balkema, Rotterdam, 461-471.

Lade, P.V. 1995. Instability of sand in the prefailure hardening regime. *Proc. First Conf on Pre-Failure Deformation Characteristics of Geomaterials,* 2:837-854.

Lade, P.V. and Duncan, J.M. 1973. Cubical triaxial tests on cohesionless soil. *Journal of the Soil Mechanics and Foundations Division,* ASCE, 99:10, 793-812.

Lade, P.V. and Prabucki, M.-J. 1995. Softening and preshearing effects in sand. *Soils and Foundations,* 35:4, 93-104.

Lee, K.L. 1965. Triaxial compressive strength of saturated sand under seismic loading conditions, PhD thesis, University of California, Berkeley.

Lee, K.L. and Seed, H.B. 1967. Drained strength characteristics of sands. *Journal of the Soil Mechanics and Foundations Division,* ASCE, 93:6, 117-141.

Luong, M.P. 1982. Stress-strain aspects of cohesionless soils under cyclic and transient loading. *International Symposium on Soil under Cyclic and transient Loading,* A. A Balkema, Rotterdam, 315-324.

FROM THE SAME PUBLISHER:

Evangelista, A. & L.Picarelli (eds) 90 5809 018 3
The geotechnics of hard soils - soft rocks – *Proceedings of the 2nd international symposium, Naples, Italy, 12-14 October 1998*
1998, 25 cm, c.2000 pp. 3v, EUR 157.50 / $185.00 / £110
Shallow and deep excavations as well as stability of natural slopes have been selected as the subjects where the most challenging problems are posed to geotechnics of hard soils and soft rocks. Considering the variety of materials, these are grouped in 3 categories, namely fine grained and coarse grained materials and weathered rocks.

Konovalov, P.A. 90 5410 722 7
Bases and foundations of buildings under reconstruction
1998, 24 cm, 240 pp.,
EUR 58.50 / $69.00 / £41 No rights India
Translation of *Osnovaniya i fundamenti rekonstruiruemikh Zadanii I,* Moscow, 1988. Revised and updated for English edition in 1996/97. Contents: Reasons for strengthening bases and foundations of buildings; Condition of bases and foundations of buildings under reconstruction; Behavioural features of foundations of in-service buildings; Reinforcement of foundations on natural base; Utilization of piles for reinforcing foundations; Stabilization of soils; Special features of construction operations related to substructure works to be carried out under reconstruction; Conclusions; References.

Maric, B., Z.Lisac & A.Szavits-Nossan (eds) 90 5410 957 2
Geotechnical hazards – *Proceedings of the XIth Danube-European conference Porec, Croatia, 25-29 May 1998*
1998, 25 cm, 906 pp., EUR 99.00/ $116.00 / £70
Topics covered are: Foundations and soil improvement, environmental geotechnics, landslides and slope stability, earthquake geotechnical engineering, earth structures and geotechnical parameters.

Ortigao, J.A.R. 90 5410 194 6
Soil mechanics in the light of critical state theories: An introduction
1995, 25 cm, 160 pp., EUR 70.00 / $82.00 / £49
St.edn: 90 5410 195 4, EUR 35.00 / $41.00 / £25
Reviews soil mechanics in the light of critical state soil mechanics. Critical state concepts gained widespread recognition as a framework to the understanding of the behaviour of soils. The same model is applicable to different materials such as sands and clays. A microcomputer program named Cris accompanies the book. It is used for training and simulation of the behaviour of soil samples subjected to triaxial tests through the critical state models. Computer program *Cris* available at: EUR 44.00 / $52.00 / £31. Hardcover edition includes computer program.

Lancellotta, R. 90 5410 178 4
Geotechnical engineering
1995, 25 cm, 448 pp., EUR 100.00 / $118.00 / £70
Student edn: 90 5410 179 2, EUR 50.00 / $58.00 / £35
Contents: Nature and composition of soils; The principle of effective stress and the state variables; Fundamentals of continuum mechanics; The porous medium: steady flow; The porous medium: transient flow; Stress-strain and strength characteristics; In-situ investigations; The collapse of soil structures; Performance and serviceability of structures; References; Index. *Warmest congratulations both to author and publisher for this first-class volume, which is a welcome contribution to the relatively rich geotechnical literature now available. *Appl.Mech.Rev. Vol.49, no.1, Jan.1996.*

Sheorey, P.R. 90 5410 670 0
Emperical rock failure criteria
1997, 25 cm, 192 pp., EUR 79.00 / $93.00 / £55
Student edn.: 90 5410 671 9, EUR 40.00/$47.00/£28
Stress analysis is carried out around the excavation in rock during the designing process. The results are then used in a failure criterion to estimate rock stability or failure. This book concentrates on emperical criteria for rocks and jointed rock masses, and their applicability to triaxial test data as well as excavation case studies. In an appendix, triaxial and polyaxial test data sets of 321 rocks are provided. Included are new closed-form interrelations between triaxial strength parameters, methods to derive an equation to Mohr's envelope, influence of rock anisotropy on all triaxial strength parameters, an anisotropic rock failure criterion and three excavation case studies with complete details. A comprehensive list of related references is given at the end of the book.

Pietruszczak, S. & G.N.Pande (eds.) 90 5410 886 X
Numerical models in geomechanics – *Proceedings of the 6th international symposium NUMOG VI, Montreal, Canada, 2-4 July 1997*
1997, 25 cm, 766 pp., EUR 124.00 / $145.00 / £87
The papers are divided in six sections: Constitutive relations for geological materials: formulation and verifications; Instability and strain localisation in geomaterials; Modelling of reinforced soil; Modelling of transient/coupled problems; Numerical Algorithms: formulation and performance; Application of numerical techniques to practical problems. Many new developments on a wide variety of topics have been reported. These include: Partially saturated soils, transition from fully to partially saturated state and vice versa, strain localistation, environmental geomechanics, parallel computing, neural networks and applications to tunnels, embankments, slopes and foundations.

All books available from your bookseller or directly from the publisher:
A.A. Balkema Publishers, P.O. Box 1675, NL-3000 BR Rotterdam, Netherlands
E-mail: sales@balkema.nl Internet: www.balkema.nl
For USA & Canada: A.A. Balkema Publishers, Old Post Rd, Brookfield, VT 05036-9704